Study of $\pi^- p \to \pi^- \eta p$ and $\pi^- p \to \pi^- \eta \eta p$ at $\sqrt{s} = 18.9$ GeV with the COMPASS experiment

I. Uman and T. Schlüter on behalf of the COMPASS collaboration

Department für Physik, Ludwig-Maximilians-Universität, Am Coulombwall 1, 85748 Garching, Germany

Abstract. The COMPASS experiment at CERN studies diffractively produced states in the light quark sector with unprecedented statistics. The observation of $f_0(1500)/f_2'(1525)$ decaying to $\eta\eta$ in 2008 data with incoming negative pion beam at 190 GeV/c poses the question whether it is produced centrally or formed by the decay of a heavier diffractively produced $\pi_1(1800)/\pi_2(1880)$. To decide, a dedicated amplitude analysis which includes different production mechanisms is formulated and compared with one which was used to fit centrally produced resonances including $f_0(1500)$ by the WA102 experiment. Unbinned mass-dependent log-likelihood fitting methods may serve to solve the ambiguities which are present in binned, mass-independent partial wave analyses.

Keywords: 13.25.-k,13.85.-t,14.40.Be,29.30.-h
PACS: hadron spectroscopy, light meson spectrum, gluonic excitations, exotic mesons, hybrids

INTRODUCTION

The study of $\pi^- p \to \pi^- \eta p$ and $\pi^- p \to \pi^- \eta \eta p$ with the COMPASS experiment can address fundamental questions about the exotic hybrid states and the candidates of the lightest *glueballs* . Both reactions are indeed very selective. The two-body systems can only populate states with $J^{PC} = even^{++}$, f-mesons decaying to $\eta\eta$, and a-mesons decaying to $\eta\pi^-$. The $\eta\eta$ states may contain admixtures of low lying 0^{++} and 2^{++} glueballs, and the $\eta\pi^-$ system may include states with non-$q\bar{q}$ quantum numbers J^{PC}, such as the 1^{-+} hybrids.

Evidences for resonant behavior of the $\eta\pi$ P-wave with $J^{PC} = 1^{-+}$ was found in the E852 experiment in the reaction $\pi^- p \to \eta\pi^- p$ at 18 GeV/c [1] and in the CBAR experiment in $\bar{p}d$ annihilation at rest in $\pi^-\pi^0\eta p_{spectator}$ [2]. The resonant nature of this wave however was questioned by an independent analysis [3] where the attempts to describe the mass dependence of the amplitude and phase motion with respect to the D wave as a Breit-Wigner resonance were problematic. More recently, the 1^{-+} exotic was confirmed in the $\eta\pi$ system by the E852 collaboration [4], however with a mass of $1257 \pm 20 \pm 25$ MeV which is below the average 1376 ± 17 MeV of the previous observations. In addition, the CBAR collaboration could not exclude the possibility that the phase variation required in the fit could be introduced through threshold effects due to the opening of the $f_1(1285) - \pi$ or $b_1(1235) - \pi$ channel [5].

The existence of glueballs is even more controversial. Glueballs can have indeed the same quantum numbers as conventional mesons. The observation of the $f_0(1500)$, supernumerary to $f_0(980)$ and $f_0(1370)$, which were believed to be, respectively, the $n\bar{n}$ and $s\bar{s}$ members of the lightest scalar nonet along with $a_0(980)$ and $K_0(1430)$, was the first indication of the presence of a state with gluonic degrees of freedom. The observation of the additional $a_0(1450)$ in line with the mass of the $K_0(1430)$ and of $f_0(1710)$ with a strong decay branching in $K\bar{K}$ along with the reinterpretation of $a_0(980)$ and $f_0(980)$ as cusps or members of a *tetraquark* nonet, led to the assignment of $f_0(1370)$ and $f_0(1710)$ as the $n\bar{n}$ and $s\bar{s}$ members, respectively. However, theoretical *flavor blind* decays of a pure glueball state deviate from the observed decay branching fractions of $f_0(1500)$ into $\pi\pi$, $K\bar{K}$, $\eta\eta$, $\eta\eta'$, $\eta'\eta'$, ... To explain this, a more general hypothesis where glueball and eventually tetraquarks can mix with ordinary mesons with the same J^{PC} was proposed. The decay branching fractions which are mainly used as a reference for this mixing scheme are taken from the results of the WA102 experiment at CERN with incoming proton beam at 450 GeV on a proton target [6].

Since in the COMPASS experiment the incoming beam energy of 190 GeV is in between the one of E852 (18 GeV) and of WA102 (450 GeV), both diffractive dissociation and central production are accessible. COMPASS can verify with much higher statistics the results of both E852 and WA102 experiments. Preliminary results of the reconstruction of exclusive, $\pi^- p \to \pi^- \eta(\eta) p$ final states with 2008 data and the formalism for the amplitude analysis will be discussed.

DETECTOR DESCRIPTION

The COMPASS NA58 experiment is a 50 meter long, high acceptance, two-stage spectrometer, located at the CERN north area of the Super Proton Syncroton which provides high intensity proton beams, secondary $5 \cdot 10^6\ s^{-1}$ hadrons and tertiary $4 \cdot 10^7\ s^{-1}$ polarized muons, with momenta up to 300 GeV/c.

The first stage, the large angle spectrometer, detects low-energetic produced particles and consist of a magnet with a bending power of 1 Tm (SM1), a tracking system, a RICH (Ring Imaging Cherenkov) detector, 1500 channel electromagnetic calorimeter (ECAL1) and a hadronic calorimeter (HCAL1).

The second stage, the small angle spectrometer more downstream, covers the medium and high energy range, consists of a higher bending power magnet of 4.4 Tm (SM2) with an additional tracking system, a second 3068 channel electromagnetic calorimeter (ECAL2) and a second hadronic (HCAL2) calorimeter.

At 190 GeV the incoming negative beam consists of π(93%), K(2.5%), μ(3%), $\bar{p}$ (0.6%) and e^-(0.1%) while the incoming secondary positive beam consists mainly of protons and pions. To identify the incoming beam particles two Cherenkov differential counters with achromatic ring focus (CEDAR) are placed upstream in the beam line. In the 2008 and 2009 setups the 40 cm long liquid hydrogen target was surrounded by two concentric rings of scintillators (RPD) which are used to identify recoiling protons by TOF and dE/dx measurements. In addition, in the very small tracking area a set of silicon microstrip detectors cooled to cryogenic temperatures and new GEM detectors with pixel readout were used in the 2008 and 2009 run.

The performance of the calorimeters has been improved with respect to the pilot run in 2004. Prior to the runs of 2008 and 2009, the two calorimeters were upgraded. In ECAL2 the central lead glass cells were replaced by 900 radiation-hard Shashlyk blocks and since 2008 new ADC with 32 sample converters were used to measure the cluster time. Because of radiation damage the optical properties of the cells deteriorate and aging may gradually change the overall response of the calorimeter, therefore LASER and LED monitoring system were implemented in 2008 and 2009, for ECAL1 and ECAL2, respectively.

DATA SELECTION

About 28% and 42% of the 2008 DATA with incoming beam at 190 GeV were processed to select $\pi^- p \to \pi^- \eta p$ and $\to \pi^- \eta\eta p$, respectively. Of those, 74% were recorded with a trigger dedicated to select diffractively and centrally produced resonances. To reduce the small component of incoming beam with negatively charged kaons the CEDAR detectors have been used. To ensure an interaction in the liquid hydrogen target, at least one primary vertex within the target container has been requested. In order to reduce the main source of *pile-up* due to elastic scattering, events with only one outgoing track with energy less than 180 GeV, associated to the outgoing charged pion, have been selected. The η mesons are identified by their decay into two photons, therefore exactly 2 and 4 clusters to select one and two η, respectively, in both ECAL1 and ECAL2 calorimeters have been requested. Exclusivity is demanded by requesting $180 < E_{\pi^-} + E_{2\gamma(4\gamma)} < 200$ GeV under the hypothesis that the charged track is a pion and neglecting the recoiling proton, which carries a negligible fraction of the incoming beam energy. Photon momenta are calculated assuming that they originated from the primary vertex. One track in the RPD is requested and is associated to the recoiling proton and the difference between the azimuthal angle of this track and the $\pi^- 2\gamma(4\gamma)$ system was chosen to be in the range between $-0.3 < \phi_{\pi^- 2\gamma(4\gamma)} - \phi_p - \pi < 0.3$ rad. To reduce the combinatorial background in the $\eta\eta$ mass range which is mainly due to the wrong combination of the good $\pi^0\pi^0$ signal, events which have at least one $\gamma\gamma$ invariant mass combination in $100 < m_{\pi^0} < 170$ MeV were rejected. The η mass reconstruction is in agreement with the PDG value [7] for both channels as can be seen in Fig. 1(left and center).

The remaining events pass the η mass constraint fit in the $\pi^- p \to \pi^- \eta p$ channel and at least one of the three possible combination passes the 2η mass constraints, in the $\pi^- p \to \pi^- \eta\eta p$ channel, with probabilities $> 10\%$.

In the 2-body channel the $\pi^-\eta$ system shows a strong peak around 1.3 GeV which can be associated to $a_2(1320)$ (Fig. 1(right)).

In the $\pi^-\eta\eta$ system a strong peak around 1.8 GeV can be observed (Fig. 2(left)). It is presumably due to the $\pi(1800)$ but an admixture with $\pi_2(1880)$ cannot be excluded. In the $\eta\eta$ mass system a structure around 1.5 GeV, which can be associated to the $f_0(1500)$, is visible (Fig. 2(center)), however $f_2'(1525)$ cannot be excluded. Furthermore, for the $\eta\pi^-$ system in the 3-body channel the dominant peak is around 1 GeV and is presumably due to $a_0(980)$ while $a_2(1320)$ is less pronounced (see Fig. 2(right)) here with respect to the 2-body final state.

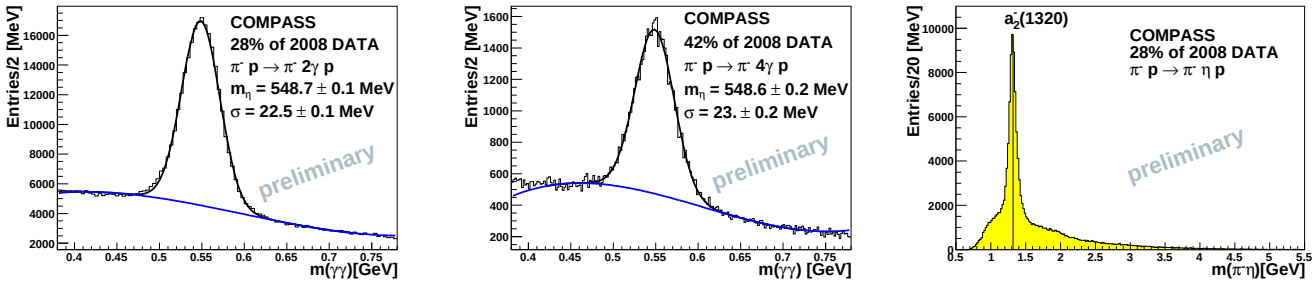

FIGURE 1. The two-photon invariant mass around the η mass in the $\pi^- p \to \pi^- 2\gamma p$ channel (left) and for the three possible combination in the $\pi^- p \to \pi^- 4\gamma p$ channel (center). Invariant mass of the $\pi^-\eta$ system (not acceptance corrected) in the $\pi^- p \to \pi^-\eta\, p$ channel (right). The nominal position [7] of $a_2(1320)$ is indicated.

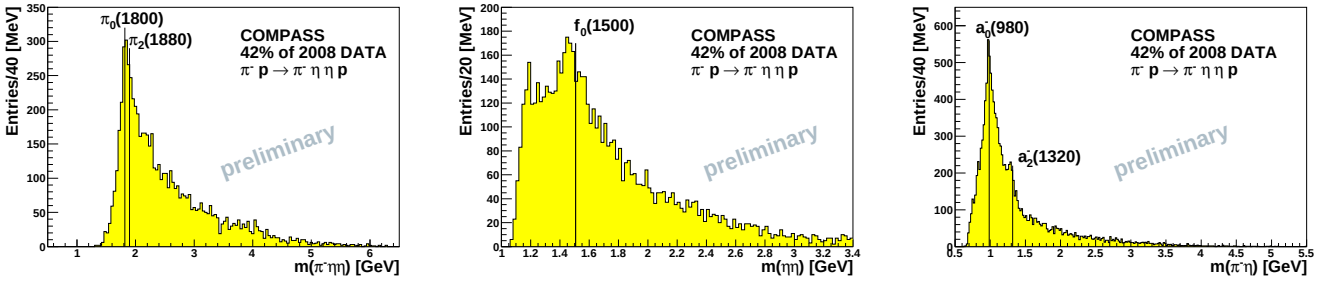

FIGURE 2. Invariant mass of the $\pi^-\eta\eta$ (left), $\eta\eta$ (center), and $\pi^-\eta$ (right) systems in the $\pi^- p \to \pi^-\eta\eta p$ channel (not acceptance corrected). The nominal positions [7] of $\pi(1800)$, $\pi_2(1880)$, $f_0(1500)$, $a_0(980)$ and $a_2(1320)$ are indicated.

AMPLITUDE ANALYSIS

For this data an independent formalism will be used. The original code was developed for the $\bar{p}p$ Crystal Barrel experiment at CERN [8] and for the E835 Fermilab experiment at Fermilab [9]. A description and adaptation of this formalism for COMPASS will be given here.

Central production is considered to be a favored reaction to produce glueballs via Double Pomeron Exchange. $f_0(1500)$ was formed centrally in the WA102 experiment and one may predict that this is also the case in COMPASS. On the other hand the presence of resonances in the other invariant mass combinations (Fig. 2(left) and 2(right)) indicates that at 190 GeV diffractive excitation coexist with central production. In addition, one cannot exclude that the $f_0(1500)$ can be also formed as a decay product of the more massive $\pi(1800)$ state which is also a non-$q\bar{q}$ candidate. The Feynmann diagrams corresponding to the central production and diffractive excitation are shown in 3(left) and 3(right), respectively. To take into consideration these possibilities the amplitude Ansatz must contain two terms, which will describe both different production processes.

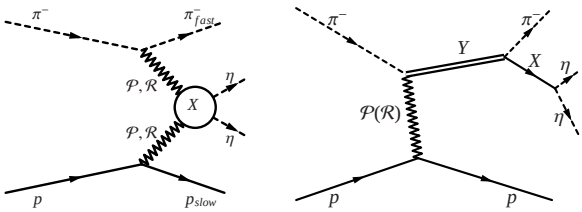

FIGURE 3. Feynmann diagram of a central production (left) and of a diffractive production (right). $\mathscr{P}$ and $\mathscr{R}$ are exchanged Pomeron or Reggeon.

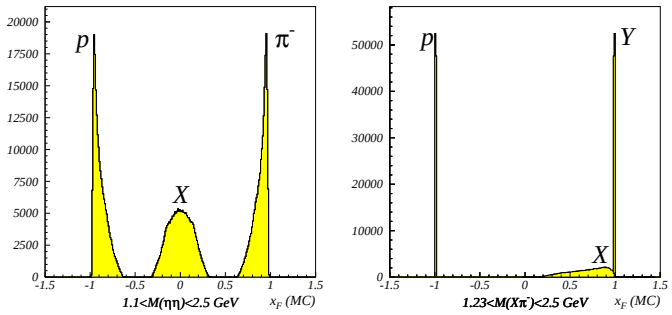

FIGURE 4. Generated x_F distributions for a reaction $\pi^- p \to \pi^- X p$ with a centrally produced resonance $X \to \eta\eta$ (left). Generated x_F distributions for a reaction $\pi^- p \to Y p$ with a diffractively produced resonance $Y \to \pi^- X$, with $X \to \eta\eta$ (right).

Production mechanism

To reproduce the average kinematics of these two processes, MC simulations have been performed [10, 11]. For a centrally produced resonance X decaying to $\eta\eta$ (Fig. 3(left)) a uniform rapidity distribution of X between -1 and 1 is assumed. The four-momentum transfer t at each vertex, t_{π^-} to the leading π^- and t_p to the recoiling p is randomized as for the case of two independent elastic vertices, i.e. as e^{-bt}, where b has a typical value of ~ 6 GeV^{-2}. Moreover $M_X^2 = -x_{P_1} x_{P_2} s$, where $x_{P_2} = 1 - x_\pi$ is the momentum fraction in the c.m of the Pomeron emitted by the π, and $x_{P_1} = x_p - 1$ is that of the Pomeron emitted by the p and s is the πp c.m. squared energy. In the case of a diffractively produced state Y with the subsequent decay into $\pi^- X$ and $X \to \eta\eta$ we assume only one exchanged Pomeron (Reggeon) (Fig. 3(left)) and $1 - x_Y = (M_Y^2 - m_{\pi^-}^2)/s$. The resulting x_F distributions of an $X \to \eta\eta$ state which is the decay product of a diffractively produced $Y \to X\pi^-$ (Fig. 4(right)) has on average higher values with respect to the one relative to a centrally produced X system decaying to $\eta\eta$ (Fig. 4(left)). At 190 GeV energy of the incoming beam the two distributions partly overlap, therefore it is not possible to fully separate these two different reactions.

Amplitude Ansatz

The decay amplitude which contains the information about the spin J of the intermediate state, is written in terms of relativistic Breit-Wigner functions for the dynamical part and spherical harmonics for the angular part as follows:

$$A^{\lambda}_{J,decay} = G_\lambda e^{i\delta_\lambda} F_J(q) \frac{Y^\lambda_J(\alpha,\beta)}{m_0^2 - s - i m_0 \Gamma(m)}. \tag{1}$$

Here λ is the component of the spin along the quantization axis, G_λ and δ_λ are the complex coupling constant and phase, $F_J(q)$ are the standard centrifugal barrier factors. A sequence of rotations of the reference frame from the beam axis, called Wick rotations, by ϕ and θ relative to the direction of flight of X and a Lorentz boost to the rest system of X and by $-\theta, -\phi$ cancel the D functions which would otherwise be needed for the first rotations. The spherical harmonic $Y^\lambda_J(\alpha,\beta)$ are calculated in this reference frame, with the angles α,β defined by the direction of one of the decay products of the resonance X with respect to the beam direction and production plane. The intensity of two resonances with masses m_0 and m_1, spin J and J' is given by

$$w_{decay}(m_0,m_1) \quad = \quad \sum_\lambda [|A^\lambda_{X_J}(m_0)|^2 + |A^\lambda_{Y_{J'}}(m_1)|^2 + 2c_\lambda \Re(A^\lambda_{X_J}(m_0) A^{\lambda *}_{Y_{J'}}(m_1)], \tag{2}$$

where $-1 \le c_\lambda \le 1$ is the degree of coherence. As we have seen the above production amplitude depends on t_1, t_2, x_1, x_2 for central production and on t and x for diffractive scattering for exchanged Pomerons (Reggeons):

$$w_{prod} = c_{CP} f(t_1,t_2,x_1,x_2) + c_{DS} f(t,x), \tag{3}$$

where c_{CP} and c_{DS} are the coupling constant for central production and diffractive scattering, respectively. The total intensity is fitted minimizing the negative log-likelihood:

$$-ln\mathscr{L} \quad = \quad -\sum_{j=1}^{N} ln(w_j) + Nln\left(\sum_{i=1}^{M} w_i\right), \tag{4}$$

with N the number of data events and $w_j \equiv w_{j,decay}$, M the number of MC events and $w_j \equiv w_{j,prod}$, i.e. the MC generation takes into account the production processes as above and with a phase space decay, while the decay process is fitted with eq. 2 only. The MC events are generated according to the ratio c_{CP}/c_{DS} which is optimized according to the observed t and x_F distributions.

The masses and widths of well established resonances are kept fixed at PDG values. $G_\lambda, \delta_\lambda, c_\lambda$ are the free parameters of the fit. Unknown resonance parameters are optimized repeating the previous free fit around the predicted mass and width and for different spin hypotheses. In standard PWA of E852 and WA102 data the fitting procedure is divided in two steps: firstly, the data are divided in small mass bins, which have typically a size of 0.04 GeV, and the angular distributions are fitted independently of the mass. Secondly, the resulting waves with the same J^{PC} in each bin are grouped together in a mass dependent fit over the full mass range, in order to determine the mass and width of the resonances with the same J^{PC}. In this amplitude analysis, instead, the negative log-likelihood which is minimized includes the full amplitude with both its angular and dynamic parts. This high constraint mass dependent fit may reduce the number of non mathematical ambiguities and/or discontinuities which are present in lower constraint standard PWA fits.

Another difference with the standard formalisms is the introduction of an additional degree of coherence which takes into account, not only the incoherence between natural and unnatural-parity exchanges in the reflectivity basis, but also a partial coherence of possible intermediate states produced both centrally and diffractively.

CONCLUSION AND OUTLOOK

Preliminary invariant mass distributions indicate the presence of $a_0(980)$, $f_0(1500)$ and $\pi(1800)$ in $\pi^- p \to \pi^- \eta(\eta) p$ which are considered non-$q\bar{q}$ candidates. A dedicated amplitude analysis has been formulated to determine not only the quantum numbers of these states but also to disentangle the different production mechanisms. The Monte Carlo studies have shown the equivalence of this formalism with the one used by previous experiments [10]. After reconstructing the more recent 2009 data taken on a liquid hydrogen target, both 2008 and 2009 data sets will be combined for the amplitude analyses.

ACKNOWLEDGMENTS

This work is supported by the German Bundesministerium für Bildung und Forschung, the LMU Universität München and the DFG Cluster of Excellence *Origin and Structure of the Universe* .

REFERENCES

1. D. R. Thompson, et al., *Phys. Rev. Lett.* **79**, 1630–1633 (1997), hep-ex/9705011.
2. A. Abele, et al., *Phys. Lett.* **B423**, 175–184 (1998).
3. A. R. Dzierba, et al., *Phys. Rev.* **D67**, 094015 (2003), hep-ex/0304002.
4. G. S. Adams, et al., *Phys. Lett.* **B657**, 27–31 (2007), hep-ex/0612062.
5. A. Abele, et al., *Phys. Lett.* **B446**, 349–355 (1999).
6. D. Barberis, et al., *Phys. Lett.* **B479**, 59–66 (2000), hep-ex/0003033.
7. C. Amsler, et al., *Phys. Lett.* **B667**, 1 (2008).
8. C. Amsler, et al., *Phys. Lett.* **B639**, 165–171 (2006).
9. I. Uman, et al., *Phys. Rev.* **D73**, 052009 (2006), hep-ex/0607034.
10. The COMPASS Collaboration (2007), CERN-SPSC-2007-037.
11. I. Uman, "The Hadron Program at COMPASS," Submitted to Chinese Physics C, 2010.